

Published in final edited form as:

J Dermatol Sci. 2010 August ; 59(2): 98–106. doi:10.1016/j.jdermsci.2010.04.016.

Identification and analysis of an early diagnostic marker for malignant melanoma: ZAR1 intra-genic differential methylation

Yui Shinojima^{1,2}, Tadashi Terui¹, Hiroyuki Hara¹, Makoto Kimura³, Jun Igarashi³, Xiaofei Wang³, Hiroyuki Kawashima², Yujin Kobayashi², Satomi Muroi², Satoshi Hayakawa⁴, Mariko Esumi⁵, Kyoko Fujiwara⁶, Srimoyee Ghosh⁶, Tatsuo Yamamoto⁷, William Held⁸, and Hiroki Nagase^{2,3,6}

¹Division of Cutaneous Science, Department of Dermatology, Nihon University Graduate School of Medicine, Tokyo, Japan

²Division of Cancer Genetics, Department of Advanced Medical Research Center, Nihon University School of Medicine, Tokyo, Japan

³Life Science, Advanced Research Institute for the Science and Humanities, Nihon University, Tokyo, Japan

⁴Division of Microbiology, Department of Pathology and Microbiology, Nihon University School of Medicine, Tokyo, Japan

⁵Department of Pathology, Nihon University School of Medicine, Tokyo, Japan

⁶Department of Cancer Genetics, Roswell Park Cancer Institute, Buffalo, NY, USA

⁷Department of Gynecology, Nihon University School of Medicine, Tokyo, Japan

⁸Department of Molecular Cellular Biology, Roswell Park Cancer Institute, Buffalo, NY, USA

Abstract

Background—Epigenetic changes such as aberrant DNA methylation and histone modification have been shown to play an important role in the tumorigenesis of malignant melanoma.

Objective—To identify novel tumor-specific differentially methylated regions (DMRs) in human malignant melanoma.

Methods—The aberrant methylation at 14 candidate human genomic regions identified through a mouse model study with quantitative DNA methylation analysis using the Sequenom MassARRAY system was performed.

Results—The CpG island Exon 1 region of the Zygote arrest 1 (ZAR1) gene, which is responsible for oocyte-to-embryo transition, showed frequent aberrant methylation of 28 out of 30 (93%) melanoma surgical specimens, 16 of 17 (94%) melanoma cell lines, 0% of 4 normal human epidermal melanocyte (NHEM) cell lines, 0% of 10 melanocytic nevi and 100% of 51 various cancer cell lines. According to the real-time RT-PCR, the ZAR1 gene was overexpressed in part of

Correspondence author: Hiroki Nagase, Division of Cancer Genetics, Department of Advanced Medical Research Center, Nihon, University School of Medicine, Tokyo, 173-8610, Japan. Phone: +81-3-3972-8337, FAX: +81-3-3972-8337, nagase.hiroki@med.nihon-u.ac.jp.

Publisher's Disclaimer: This is a PDF file of an unedited manuscript that has been accepted for publication. As a service to our customers we are providing this early version of the manuscript. The manuscript will undergo copyediting, typesetting, and review of the resulting proof before it is published in its final citable form. Please note that during the production process errors may be discovered which could affect the content, and all legal disclaimers that apply to the journal pertain.

the hypermethylated cell lines, while its low expression with bivalent histone methylation status was seen in unmethylated cell lines.

Conclusion—Our findings suggest that the ZAR1 intra-genic differentially methylated region would be a useful tumor marker for malignant melanoma and may be other type of cancers. The involvement of ZAR1 in the carcinogenesis of melanoma, still remains unclear, although we have examined tumorigenic capacities by exogenous full-length ZAR1 over-expression and siRNA knock-down experiments.

1. Introduction

Malignant melanoma is relatively rare but is a leading cause of death in skin neoplasms. It is a highly aggressive tumor and only a small number of patients with metastatic melanoma survive for five years [1]. Most melanomas often do not respond to chemotherapy and radiotherapy, and its incidence rates have been increasing for the last 30 years [1]. It is often difficult to histologically determine whether melanocytic lesions are benign or malignant. There is a frequent discordance between expert pathologists in the histopathological diagnosis of melanoma and melanocytic neoplasms [2]. Therefore, a new rapid differential diagnosis method between benign melanocytic nevi and malignant melanoma is urgently needed, in addition to a new treatment.

Many irreversible changes in DNA sequence, such as chromosomal deletions, amplifications and gene mutations, have been reported to be associated with the development and progression of melanoma [3]. However, more recently, epigenetic changes such as aberrant DNA methylation and histone modifications that do not affect DNA sequence but are stably inherited to daughter cells, that may be reversible events, have been shown to play an important role in the tumorigenesis of malignant melanoma [4]. Aberrant methylation of the promoter CpG islands of tumor-suppressor genes has been known to play an important role during cancer development. It is consistent with results in the transcriptional silencing of growth-regulatory genes [5]. At least 50 aberrant methylated genes have been identified to date that are silenced during melanoma development and progression and mainly promoter CpG island hypermethylation [4]. Some authors, however, have shown that CpG hypermethylation in non-promoter regions does not interfere with transcription and is even associated with increased or ectopic gene-expression in cancers [6-8].

Histone modifications, including acetylation, and phosphorylation, are another mechanism besides DNA methylation [9]. Acetylated histones are associated with transcriptionally active chromatin, whereas, methylation of histone proteins can result in either activation or repression [4]. However, in cancer development, histone modifications have not yet been analyzed extensively.

In this report, in order to identify new tumor-specific differentially methylated regions (DMRs) in humans, we initially performed Restriction Landmark Genomic Scanning (RLGS) comparing normal mouse skin with tumors obtained from the two-stage skin carcinogenesis mouse model induced by an aggressive two-stage chemical induction protocol to C57BL/6J inbred mice (Ghosh et al., Submitted, 2010). By using the RLGS method and virtual image RLGS *in silico* analysis, we have confirmed 58 skin tumor-specific differentially methylated regions (DMRs) in mouse models. Among those, 14 human genomic regions that had homology to mouse genomic sequences of skin tumor specific DMRs were selected and examined by quantitative analysis using base-specific cleavage and mass spectrometry. We confirmed that aberrant methylation of the off-promoter of the ZAR1 intergenic region occurs very frequently in malignant melanomas compared to nevus and normal human melanocyte cell lines. To our knowledge, this is the

first study showing aberrant methylation of ZAR1 as a candidate early-detection biomarker in human tumors, especially in malignant melanomas.

2. Materials and Methods

2.1. Animal samples

The two-stage skin carcinogenesis mouse model was induced by an aggressive two-stage chemical induction protocol to C57BL/6J inbred mice at Roswell Park Cancer Institute under the Institutional Animal Care and Use Committee approval. (Ghosh et al. submitted, 2010).

Briefly, 7,12-Dimethylbenz(a)anthracen (DMBA) is used as a carcinogen and 12-O-tetradecanoylphorbol-13-acetate (TPA) as a promoter. At 6 - 12 weeks of age, the back-skin of each mouse was carefully shaved with an electric clipper. Two days after shaving, on a Monday 200 μ l of DMBA (0.125 mg/ml) was dissolved in acetone and applied to the back of each mouse. Following five weeks of administration of DMBA every Monday and 200 μ l TPA (5×10^{-5} M) solution on every Friday the mice were treated twice weekly with the same dose of TPA for up to 20 weeks. Skin papillomas and carcinomas were collected and frozen in liquid nitrogen and later on stored at -80°C . The pathological stages of the cancers and papillomas were determined by histological sections.

2.2. Human surgical specimens and cell lines

Thirty surgical melanoma specimens, 10 from fresh-frozen and 20 from formalin-fixed paraffin embedded sections, and 10 fresh-frozen melanocytic nevus specimens were obtained from 40 patients at Nihon University School of Medicine, Itabashi Hospital, Japan, with Institutional Review Board-approved informed consents.

Malignant melanoma cell lines, G361, COLO679, CRL1579 and SK-MEL-28 were obtained from the RIKEN BioResource Center (Tsukuba, Japan). GAK, MeWo, A2058 and HMY-1 were obtained from the Health Science Research Resources Bank, Japan Health Science Foundation (Sennan, Japan). SK-MEL-2, SK-MEL-31, RPMI-7951, A-375, COLO829, HT-144, Hs 294T, Hs 695T and Hs 839.T were obtained from the American Type Culture Collection (Manassas, VA). Four independent normal human epidermal melanocyte cell lines were obtained from Cascade Biologics (Portland, OR). Another 51 various types of malignant tumor cells and three normal fibroblast cells were obtained from Roswell Park Cancer Institute (Buffalo, NY). The cells are as follows: TE1, TE2, TE3, TE4, TE5, TE7, TE8, TE9, TE11, TE12, TE13, TE15, KE3, KE6, KE8 (esophageal cancer), SK-N-D2, SK-N-SH, CHP134, NBLS, KELLY (neuroblastoma), U373, U118 (astrocytoma), A172 (glioblastoma), U251, HS683 (glioma), GOS4 (Wilms tumor), A431 (epidermoid carcinoma), NCI-H441 (lung adenocarcinoma), SK-MES-1 (lung squamous carcinoma), MCF7, MDA-MB-231 (breast adenocarcinoma), SAOS, U205 (osteosarcoma), JR-1 (rhabdomyosarcoma), ASPC, BXPC3 (pancreatic cancer), RKO, LOVO, COLO205, LS180, SW480, SW620, HT29 (colorectal cancer), RCC (Renal cell carcinoma), PC3, 22RV, LNCAP, DU145 (prostate carcinoma), J82, T24 (bladder carcinoma), HeLa-TR (cervical cancer), TR126 (tongue squamous cell carcinoma), and MRC5p30, KMp15, TSp28 (normal fibroblast).

Normal ovary samples (paraffin-embedded specimens) were obtained from three patients from the Department of Gynecology, Nihon University, Itabashi Hospital, Tokyo, Japan.

2.3. DNA and RNA extraction

DNA was extracted by the standard phenol/chloroform purification method or with a QIAamp DNA Mini Kit (Qiagen, Valencia, CA). From paraffin-embedded specimens, melanoma tissue was dissected with a scalpel from five slices of 20- μ m-thick tissue sections and deparaffinized by xylene at room temperature. DNA was extracted by the above-mentioned standard DNA purification method.

Oocytes were collected by using Leica Laser Microdissection (LMD) systems (LMD 6000, Leica Microsystems, Wetzlar, Germany). Paraffin-embedded ovary tissue was cut into 5 μ m sections with a microtome. The sections were attached to a microscope glass slide coated with foil (Leica Microsystems) and deparaffinized, followed by Hematoxylin- and Eosin-staining. Approximately 1000 oocytes from 30 glass slides per one ovary were collected in a 500 μ l ependorf tube by LMD (Fig. S1). One hundred μ l of lysis buffer with 1 μ l of salmon-sperm DNA (10mg/ml) (Invitrogen, Carlsbad, CA) was added, and DNA was extracted by the standard phenol/chloroform purification method.

The total RNA was isolated from the melanoma cell lines and normal human epidermal melanocyte cell lines using a QIA shredder (Qiagen) and RNeasy Mini Kit (Qiagen). RNA integrity and quality were assessed using an Agilent 2100 Bioanalyzer with an RNA 6000 Nano Kit (Agilent Technologies, Santa Clara, CA) according to the manufacturer's protocol.

2.4. Sequence database

The databases used for sequence analysis, BLAT, can be found on the University of California, Santa Cruz (UCSC), Genome Bioinformatics website (<http://genome.ucsc.edu/>). The human sequence was from the March 2006 release (hg18), and the mouse sequence was from the July 2007 release (mm9) of the C57BL/6J mouse strain. The February 2006 release (mm8) of the C57BL/6J mouse genome information was used for Virtual RLGs [10].

2.5. Bisulfite treatment and PCR

All primers were purchased from Operon Biotechnology (Tokyo, Japan). Bisulfite modification was performed by the sodium-bisulfite method with an EZ DNA Methylation Kit (Zymo Research, Orange, CA). The bisulfite-treated genomic DNA was amplified by HotStar Taq Polymerase (Qiagen) (15 min at 94°C followed by 45 cycles of 20s at 94°C, 30s at 56°C, and 1min at 72°C with a 3-minute final extension at 72°C). The primers are listed in Table S1. The PCR products obtained were subjected to gel electrophoresis analysis and then forwarded for Sequenom MassARRAY analysis.

2.6. Quantitative analysis of DNA methylation using base-specific cleavage and Matrix-Assisted Laser Desorption/Ionization Time-of-Flight Mass Spectrometry (MALDI-TOF MS)

A Sequenom MassARRAY quantitative methylation analysis using the MassARRAY Compact System (Sequenom, San Diego, CA) was performed for the quantitative DNA methylation analysis. This system is based on MS for the detection and quantitative analysis of DNA methylation using homogeneous MassCLEAVE (hMC), base-specific cleavage and MALDI-TOF MS [11]. Bisulfite treatment produces methylation-dependent sequence variations of C to T in the amplification products. These C/T variations appear as G/A variations in the cleavage products generated from the reverse strand by base-specific cleavage. These G/A variations result in a mass difference of 16Da per CpG site, which is detected by the MassARRAY system. In the mass spectrum, the relative amount of methylation can be quantitated by comparing the signal intensity between the mass signals of methylated and non-methylated templates, as described before [11]. Briefly, genomic DNA (1 μ g) was converted with sodium bisulfite using the EZ DNA methylation kit (Zymo Research, Orange, CA). The primers were designed using Methprimer

(<http://www.urogene.org/methprimer/index1.html>) or Methyl Primer Express ® Software v1.0 (Applied Biosystems, Foster City, CA), and are listed in Table S1. The primer pairs were designed to span the DMRs closely adjacent region or GC rich region as indicated. Bisulfite-treated DNA (~20 ng/ml) was amplified using HotStar Taq Polymerase (Qiagen) in a 5 µl reaction volume using PCR primers at a 200 nM final concentration. After Shrimp Alkaline Phosphatase treatment, 2 µl of the PCR products were used as a template for *in vitro* transcription and RNase A Cleavage for the T-reverse reaction, as per the manufacturer's instructions (Sequenom hMC). The samples were desalted and spotted on a 384-pad SpectroCHIP (Sequenom) using a MassARRAY nanodispenser, followed by spectral acquisition on a MassARRAY Analyzer Compact MALDI-TOF MS (Sequenom). The resultant methylation calls were performed by EpiTYPER software v1.0 (Sequenom) to generate quantitative results for each CpG site or an aggregate of multiple CpG sites.

A standard curve of quantitative DNA methylation analysis was performed by using 0%, 50% and 100% methylated samples. A 5-aza-2'-deoxycytidine (5-Aza-dC) treatment was performed twice (days 1 and 3) in a standard normal lymphocyte cell culture and cells were harvested on day 4 for DNA preparation of the 0% methylation samples. Twice M.sss-1-treated DNA was prepared according to the manufacturer's protocols (New England Biolabs, Beverly, MA) at 37°C for 1h followed by 65°C for 20 min inactivation for 100% methylation samples. An equal amount mixture was used for 50% methylation samples. A standard curve was fitted and methylation levels were adjusted. The experiment was performed in triplicate. The non-applicable reading and its corresponding site were eliminated in calculation.

2.7. Bisulfite direct sequence analysis

The bisulfite-treated DNA was also directly sequenced on an Applied Biosystems 3130xl Genetic Analyzer using a BigDye Terminator v3.1 Cycle Sequencing Kit, following the manufacturer's instructions (Applied Biosystems).

2.8. Quantitative real-time reverse transcription-PCR

The mRNA expression level was analyzed by quantitative real-time reverse transcription-PCR (qRT-PCR). Total RNA was extracted using the previously mentioned method. Single-strand cDNA was synthesized from total RNA using Prime Script RT Reagent Kit (Takara Bio, Japan). The generated cDNA was amplified on a Thermal Cycler Dice® Real-Time System (Takara Bio, Japan) using SYBR Premix Ex Taq (Takara Bio, Japan). The primer sequences and annealing temperatures are as follows: ZAR1-F: 5'-ATGTGTGGTGTGTACAGGGAAC-3', ZAR1-R 5'-TTTTACTGGGCAGGAACATCTC-3'; T_m 60°C. The resulting PCR cycle-time (Ct) values were collected using the software provided for the Thermal Cycler Dice® Real-Time System. The expression level of the glyceraldehydes-3-phosphate dehydrogenase (GAPDH) gene was measured by using GAPDH-F: 5'-GCACCGTCAAGGCTGAGAAC-3' and GAPDH-R: 5'-TGGTGAAGACGCCAGTGGA-3' primers at an annealing temperature of 60°C and was normalized to the amount of input cDNA. The experiments were performed in triplicate.

2.9. Chromatin Immunoprecipitation (ChIP) Assay

Five melanoma cell lines (HT-144, A2058, MeWo, SK-MEL-31 and Hs 839.T) and one normal human epidermal cell lines (NHEM-D) were cross-linked in 1% formaldehyde at 37°C for 10 min. Cell lysates were resuspended in lysis buffer and shredded to generate DNA fragments of 200-1,000 base pairs using the Bioruptor. Chromatin immunoprecipitation was performed according to the manufacturer's protocols (Upstate, Billerica, MA). Cross-links were reversed at 65°C, and DNA was extracted by phenol/chloroform purification and ethanol precipitation.

Histone H3 (dimethyl K4) antibody (Abcam, Cambridge, England), Histone H3 (trimethyl K4) antibody (Abcam), Trimethyl-Histone H3 (K27) antibody (Upstate) and Rabbit Control IgG (Abcam) were used.

To determine the presence of specific genomic DNA sequences obtained from ChIP DNAs, qRT-PCR using the immunoprecipitated fragment DNA was performed as described before. For the qRT-PCR of ZAR1 promoter, forward 5'-CGGGCAAGTCGCCTATTTA-3' and reverse 5'-AACACGTAACCGTCCAGCAC-3' primers were used and an annealing temperature of 60°C was chosen. For the qRT-PCR of the ZAR1 Exon 1, primers of 5'-CACAAGTGAAGTTCGGAGCA-3' and 5'-CTGACCAGAATCCCAGCAGT-3' were synthesized and an annealing temperature of 60°C was used. The experiments were performed in triplicate.

3. Results

3.1. Novel genes with tumor-specific DMRs identified by the RLGS method

We used the RLGS method to identify a novel genomic region with aberrant methylation in the mouse-skin cancer model, and identified 510 loci that are differentially methylated in skin cancer and normal skin samples (Ghosh et al., Submitted, 2010). Among 510 spots, 58 spots were identified using the database of virtual RLGS [10]. We found that 14 homologous regions of mouse-skin tumor-specific DMRs showed a high conservation between the two species (Table 1), because the other regions showed neither the conserved genomic structure between two species, CpGi structure, intra-genic region nor consistent amplified fragments by bisulfite PCR reaction in some reason.

3.2. Methylation status of homologous regions of mouse-skin tumor-specific DMRs in human melanomas

To determine the methylation status of homologous regions of mouse-skin-tumor-specific DMRs in human melanoma, we performed an analysis using the Sequenom MassARRAY method and evaluated the methylation profiles of 14 genes in 10 fresh-frozen melanoma surgical specimens, 17 melanoma cell lines, and three normal human epidermal melanocyte cell lines. The results of a Sequenom MassARRAY analysis of the human orthologous genomic regions are summarized in Table S2.

In the *ZAR1* gene (RLGS spot 5D52), a significant difference in methylation was seen between a surgical melanoma specimen and normal melanocyte cell lines. The Sequenom MassARRAY *ZAR1* data are shown as an epigram in Fig. 1.

To confirm the DNA methylation *ZAR1* data identified by MassARRAY EpiTYPER, an additional direct bisulfite sequence analysis was performed using two melanoma surgical specimens, four malignant melanoma cell lines (A375, COLO679, GAK and RPMI7951), and two normal human epidermal melanocyte cell lines (NHEM-M and NHEM-D). Direct bisulfite sequence analysis also showed agreement with the data from the MassARRAY EpiTYPER. Representative data on the direct bisulfite sequence of GAK (melanoma) and NHEM-D (normal melanocyte) are shown in Fig. S2.

3.3. DNA methylation status of the DMR within the ZAR1 gene

We further analyzed an additional 20-melanoma tissues obtained from paraffin-embedded sections, 10 fresh-frozen melanocytic nevus specimens and one normal human epidermal melanocyte cell line by MassARRAY EpiTYPER.

In order to analyze melanoma tissues and microdissected oocytes obtained from the paraffin-embedded sections, we prepared a primer set designed for 191 bp of the bisulfite-treated fragment (ZAR1-S-F and ZAR1-S-R: Table S1) for MassARRAY EpiTYPER. In the *ZAR1* gene, a very high frequency of aberrant methylation was observed in 28 out of 30 surgical specimens, 16 of 17 malignant melanoma cell lines, 0 of four normal human epidermal melanocyte cell lines and none of the melanocytic nevus surgical specimens (Fig. 2).

We next analyzed the methylation status of *ZAR1* in the other 51 various types of malignant tumor cell lines, three nontumorigenic fibroblast cell lines and three microdissected oocyte specimens from three independent ovaries. High methylation levels were seen in all the malignant tumor cell lines and three oocyte specimens, while low methylation level was seen in all three nontumorigenic fibroblast cell lines (Fig. S3).

3.4. Analysis of ZAR1 expression

To determine whether the gene-expression pattern of *ZAR1* is associated with the methylation patterns, we prepared RNA from 17 melanoma cell lines and four normal human epidermal melanocyte cell lines and analyzed mRNA levels by quantitative real-time reverse transcription-PCR (qRT-PCR). By this analysis, contrary to our expectations, the downstream gene in seven out of 16 hypermethylated malignant melanoma cell lines, showed a more-than-two fold increase of expression in respect to the normal melanocyte cell line of HEMa-LP, while its expression and CpG methylation level were low in all of the hypomethylated cell lines, including an Hs 839.T malignant melanoma cell line and four epidermal melanocyte cell lines (Fig. 3). RNA degradation was analyzed by using the Agilent 2100 Bioanalyzer and was detected in none of the cell lines, including *ZAR1*-expressing cells (Fig. S4).

In 18 out of 51 various malignant tumor cell lines, the downstream gene also showed a more-than-two fold increase of expression, while all three normal fibroblast cells did not show any detectable expression (Fig. S5).

3.5. Methylation status of whole sequence of the ZAR1 CpG island

The human homologous region of RLGS spot 5D52 within the mouse *Zar1* gene is located 380 bp downstream of the transcription initiation site and in the middle of the first long exon. Aberrant methylation was initially detected in this region, where Exon1 and a part of intron 1 is located within a CpG island with 168 CpGs including the *ZAR1* promoter region. We examined the methylation levels of the entire 1,472 bp of the CpG island by using the MassARRAY EpiTYPER.

Two surgical melanoma specimens (YS1004 and YS1005) and two melanoma cell lines (HT-144 and HMY-1), that showed high *ZAR1* expression, and two normal human epidermal melanocyte cell lines (NHEM-L and NHEM-D), that have low *ZAR1* expression, were analyzed in this experiment.

At the promoter region, DNA was methylated in neither the melanoma nor the normal melanocyte, while the downstream region, including Exon 1 of *ZAR1*, showed a distinct methylation pattern between melanoma (high methylation level) and normal melanocyte (low methylation level) (Fig. 4).

3.6. Chromatin Immunoprecipitation (ChIP) Assay for Histone modification antibodies

The mRNA expression analysis and methylation status of the whole CpG island suggested that other epigenetic alterations might also be involved in the expression of *ZAR1*, such as

histone modifications. To determine whether histone modifications are associated with the gene-expression of ZAR1, we performed chromatin immunoprecipitation (ChIP) coupled with detection by qRT-PCR in the promoter region and the Exon 1 region of ZAR1 using histone modification antibodies. The cells derived from three different types used for ChIP: (i) high expression levels of ZAR1 mRNA with DNA methylation (HT-144 and A2058, malignant melanoma cell lines), (ii) low expression levels of ZAR1 mRNA with DNA methylation (MeWo and SK-MEL-31, malignant melanoma cell lines), (iii) low expression levels of ZAR1 mRNA with demethylation (Hs 839.T, malignant melanoma cell line and NHEM-D, melanocyte cell line).

We examined histone modification by the ChIP assay using H3K4me2, H3K4me3 and H3K27me3 antibodies. A high level of the presence in the immunoprecipitated DNA using the H3K27me3 antibody indicating repressive histone modification was detected at the ZAR1 promoter region and Exon 1 in the group (iii) cells that express low level of ZAR1 mRNA, while the H3K27me3 did not present in melanoma cells that express a high level of ZAR1 mRNA (Fig. 5A and 5B).

In contrast, the active histone modifications H3K4me2 and H3K4me3 levels were high at the promoter region in all three groups (Fig. 5A), while at the Exon 1 region the level is high in group (iii) cells that express a low level of ZAR1, but low in melanoma cells that express a high level of ZAR1 (Fig. 5B).

4. Discussion

We performed the MassARRAY EpiTYPER analysis to determine the quantitative level of DNA methylation in malignant melanoma at the CpG sites of 14 conserved human genomic regions that are homologous to mouse-skin tumor-specific DMRs to identify new candidate melanoma tumor-related genes. Among the 14 genomic regions, we identified an extremely high frequency of aberrant methylation at a ZAR1 Exon1 CpG island in malignant melanomas as well as many other type of cancer cell lines. Most study for assessment of DNA methylation as focused on promoter CpG island methylation, and has been analyzed only for a restricted set of CpG sites in their target regions. Thus, one must extrapolate to estimate the degree of methylation in the whole region [11]. In this study, we initially used the RLGS method to identify mouse DMRs and then confirmed them by MassARRAY EpiTYPER. The RLGS method can quantitatively analyze the methylation status at the *NotI* sites of global genomic regions, including the regions outside the promoter. MassARRAY EpiTYPER, which analyzes the methylation level by base-specific cleavage in combination with MALDI-TOF-MS detection, has enabled us to access the quantitative measurement in methylation at each CpG unit in large stretches of genomic DNA, where fractions with at least 5% methylated DNA can be detected in mixtures [11]. Therefore, we could detect a differentially methylated region in the exon of ZAR1 that has never been identified as an aberrant methylated region in clinical tumor samples.

ZAR1 is an ovary-specific maternal factor that plays essential roles during the oocyte-to-embryo transition [12]. The mouse and human ZAR1 proteins contain 361 and 424 amino acids, respectively, and share 59% amino acid identity. ZAR1 is also evolutionarily conserved in vertebrate ovaries since orthologs were cloned in rat, frog, zebrafish, and pufferfish [13]. ZAR1 expression was reported to be restricted to the ovaries in mice, and to the ovaries and testes in humans [12]. Although the ZAR1 protein is not a member of any previously characterized proteins families, it does contain an atypical Plant Homeo Domain (PHD) finger in its C terminal. PHD domains are found in two major classes of proteins: (i) transcriptional activators, repressors or cofactors and (ii) subunits of complexes that modulate chromatin. Thus, ZAR1 may be a transcriptional regulator, and the conserved

ZAR1 C terminus is probably functionally important through PHD-histone interaction. This is the first report that ZAR1 mRNA expression is up-regulated in tumors, suggesting its role in tumorigenesis (See Fig. 3).

Most studies in cancer have emphasized promoter CpG island hypermethylation and silencing of tumor-suppressor gene-expression. However, our results indicate that tumor-specific DNA methylation of CpG islands located downstream of the promoter region is positively associated with ZAR1 gene-expression, and suggested that other epigenetic alterations such as histone modifications might also be involved in the expression of a possible histone-interacting protein.

In general, acetylated histones are associated with transcriptionally active chromatin, whereas, methylation of histone proteins can result in either activation or repression [4]. To confirm other epigenetic alterations, we first searched for chromatin modifications of the ZAR1 region using the database from CHIP-Sequencing analysis, which can be found on the UCSC Genome Bioinformatics website. In benign cell lines (GM12878, HUVEC and NHEK), H3K4me2, H3K4me3 and H3K27me3 levels were high ranging from the promoter to Exon 1 of ZAR1, while in malignant B-cell lymphoma cell line (K562), its levels were low. In methylated histone, histone H3 lysine 4 (H3K4) and lysine 27 (H3K27) methylation play an important role in gene-expression. H3K4 methylation is associated with actively transcribed genes [14,15], while H3K27 methylation negatively regulates transcription by promoting a compact chromatin structure [16]. However, a recent study revealed a specific modification pattern, termed bivalent domains, consisting of H3K4 methylation and H3K27 methylation in embryonic stem (ES) cells [17]. Bivalent domains are associated with low levels of gene-expression [17]. Because of the above-mentioned studies, we performed a CHIP assay using H3K4me2, H3K4me3 and H3K27me3 antibody and demonstrated the presence of H3K27me3 at the ZAR1 promoter region in melanoma and normal melanocyte cells that express low levels of ZAR1 mRNA. It did not present in melanoma cells that express a high level of ZAR1 mRNA, and H3K4me2 and H3K4me3 did present at the promoter region in all cells. Taken together, these results suggest that both the DNA methylation of Exon 1 and low levels of H3K27me3 might be necessary for the over-expression of ZAR1; moreover, its promoter might be simultaneously modified by both repressive and activating histone methylation events in normal and tumor cells, resulting in repression of mRNA expression, as seen in the bivalent domain in ES cells.

Frequent aberrant methylation and over-expression of ZAR1 suggested its direct relationship to carcinogenesis. We therefore performed analyses of full-length ZAR1 cDNA plasmid transfection for normal melanocytes and siRNA targeting ZAR1 transfection for melanoma cells, but no difference in either cell growth rate or morphology of the transfected cells were observed (Fig. S6). These accumulating negative results of functional roles of ZAR1 protein in carcinogenesis suggest that this ZAR1 intra-genic aberrant methylation may be assumed to be a secondary effect of the carcinogenesis process or the primary effect resulting in the regulation of another genetic event(s).

In conclusion, we identified a frequently aberrant methylated region within the Zygote arrest 1 (ZAR1) gene in melanoma, and demonstrated a distinct methylation pattern between melanoma and nevus; therefore, the aberrant methylation of ZAR1 may be a useful tumor biomarker to distinguish nevus from melanoma for early diagnosis. In addition, this study suggested that immediate diagnosis by analyzing the aberrant methylation of ZAR1 after excising skin tumors that are difficult to differentiate from melanoma may reveal a decrease in the incidence of progressive melanomas after surgery, because almost all melanomas are treatable by surgical removal during the early stages of development. It is not possible to determine clearly whether or not ZAR1 is directly related to carcinogenesis from this study;

however, this report suggests that the aberrant methylation of the ZAR1 gene may be one of the best biomarkers for melanoma diagnosis. Further studies will be needed to define the role of ZAR1 Exon 1 DNA methylation in tumorigenesis.

Supplementary Material

Refer to Web version on PubMed Central for supplementary material.

Acknowledgments

We thank Ms Kahoru Tagata and Paula Jones for administrative support. This work was supported by a Nihon University Multidisciplinary Research Grant (2006-2007), the Academic Frontier Project for 2006 Project for Private Universities, a matching fund subsidy from MEXT (to Hiroki Nagase.), and the National Institute of Environmental Health Services RO1 (ES012249) to HN.

References

1. Cancer facts & figures. Atlanta: American Cancer Society; 2009.
2. Farmer ER, Gonin R, Hanna MP. Discordance in the histopathologic diagnosis of melanoma and melanocytic nevi between expert pathologists. *Hum Pathol* 1996;27:528–31. [PubMed: 8666360]
3. Chin L, Garraway LA, Fisher DE. Malignant melanoma: genetics and therapeutics in the genomic era. *Genes Dev* 2006;20:2149–82. [PubMed: 16912270]
4. Rothhammer T, Bosserhoff AK. Epigenetic events in malignant melanoma. *Pigment Cell Res* 2007;20:92–111. [PubMed: 17371436]
5. Robertson KD. DNA methylation and human disease. *Nat Rev Genet* 2005;6:597–610. [PubMed: 16136652]
6. Jones PA. The DNA methylation paradox. *Trend Genet* 1999;15:34–7.
7. Salem CE, Markl ID, Bender CM, Gonzales FA, Jones PA, Liang G. PAX6 methylation and ectopic expression in human tumor cells. *Int J Cancer* 2000;15:179–85. [PubMed: 10861471]
8. Smith JF, Mahmood S, Song F, Morrow A, Smiraglia DJ, Zhang X, et al. Identification of DNA methylation in 3' genomic regions that are associated with upregulation of gene expression in colorectal cancer. *Epigenetics* 2007;2:161–72. [PubMed: 17965620]
9. LaVoie HA. Epigenetic control of ovarian function: the emerging role of histone modifications. *Mol Cell Endocrinol* 2005;243:12–8. [PubMed: 16219412]
10. Smiraglia DJ, Kazhiyur-Mannar R, Oakes CC, Wu YZ, Liang P, Ansari T, et al. Restriction landmark genomic scanning (RLGS) spot identification by second generation virtual RLGS in multiple genomes with multiple enzyme combinations. *BMC Genomics* 2007;30:446. [PubMed: 18053125]
11. Ehrlich M, Nelson MR, Stanssens P, Zabeau M, Liloglou T, Xinarianos G, et al. Quantitative high-throughput analysis of DNA methylation patterns by base-specific cleavage and mass spectrometry. *Proc Natl Acad Sci USA* 2005;102:15785–90. [PubMed: 16243968]
12. Wu X, Viveiros MM, Eppig JJ, Bai Y, Fitzpatrick SL, Matzuk MM. Zygote arrest 1 (Zar1) is a novel maternal-effect gene critical for the oocyte-to-embryo transition. *Nature Genet* 2003;33:187–91. [PubMed: 12539046]
13. Wu X, Wang P, Brown CA, Zilinski CA, Matzuk MM. Zygote arrest 1 (Zar1) is an evolutionarily conserved gene expressed in vertebrate ovaries. *Biol Reprod* 2003;69:861–7. [PubMed: 12773403]
14. Sims RJ 3rd, Chen CF, Santos-Rosa H, Kouzarides T, Patel SS, Reinberg D. Human but not yeast CHD1 binds directly and selectively to histone H3 methylated at lysine 4 via its tandem chromodomains. *J Biol Chem* 2005;280:41789–92. [PubMed: 16263726]
15. Wysocka J, Swigut T, Milne TA, Dou Y, Zhang X, Burlingame AL, et al. WDR5 associates with histone H3 methylated at K4 and is essential for H3K4 methylation and vertebrate development. *Cell* 2005;121:859–72. [PubMed: 15960974]
16. Ringrose L, Ehret H, Paro R. Distinct contributions of histone H3 lysine 9 and 27 methylation to locus-specific stability of polycomb complexes. *Mol Cell* 2004;16:641–53. [PubMed: 15546623]

17. Bernstein BE, Mikkelsen TS, Xie X, Kamal M, Huebert DJ, Cuff J, et al. A bivalent chromatin structure marks key developmental genes in embryonic stem cells. *Cell* 2006;125:315–26. [PubMed: 16630819]

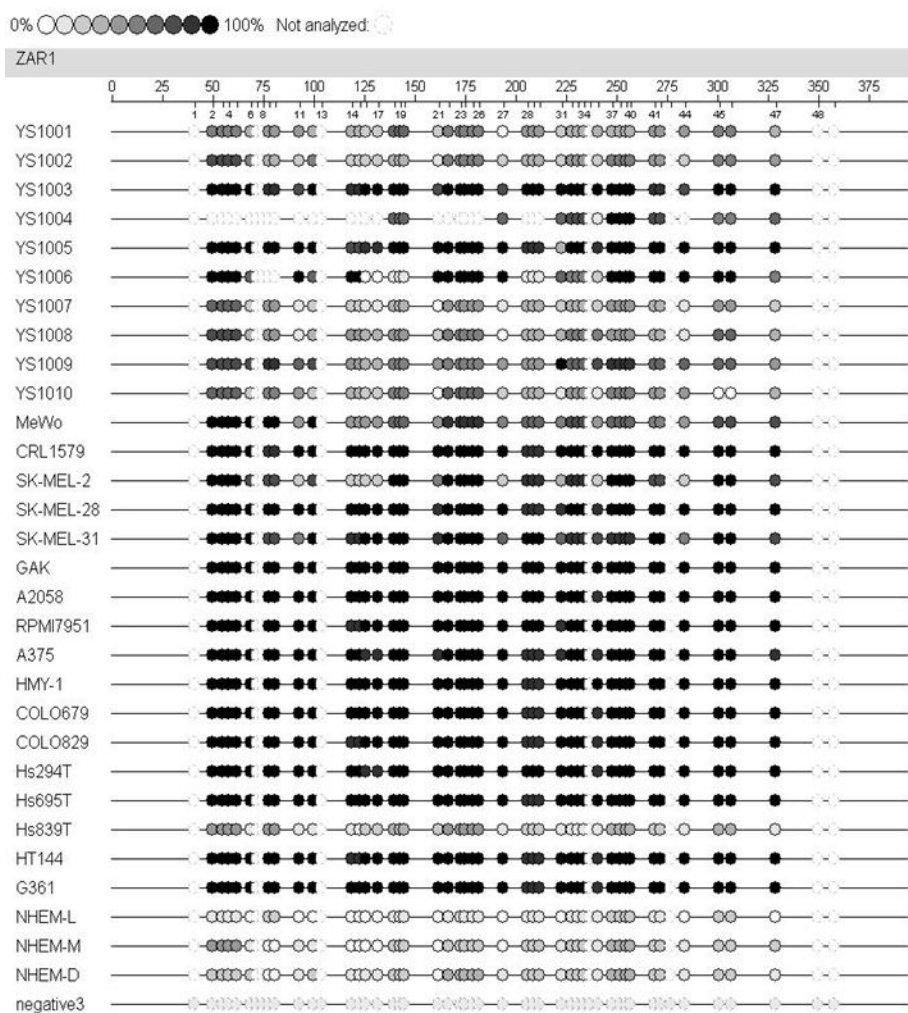


Fig. 1. Sequenom MassARRAY analysis of the percentage of DNA methylation in the human homologous genomic region of RLGS spot 5D52 (Zar1). The EpiTYPER program from Sequenom MassARRAY analysis provides the results of the percent of methylation as an epigram. The epigram shows the percentage of DNA methylation level of each CpG site of the target region. Different colors display relative methylation changes in 10% increments. The black circle indicates 100% methylation, and the white circle is 0% methylation at each CpG site. The number of CpG sites, target-sequence length and sample names are included in each epigram.

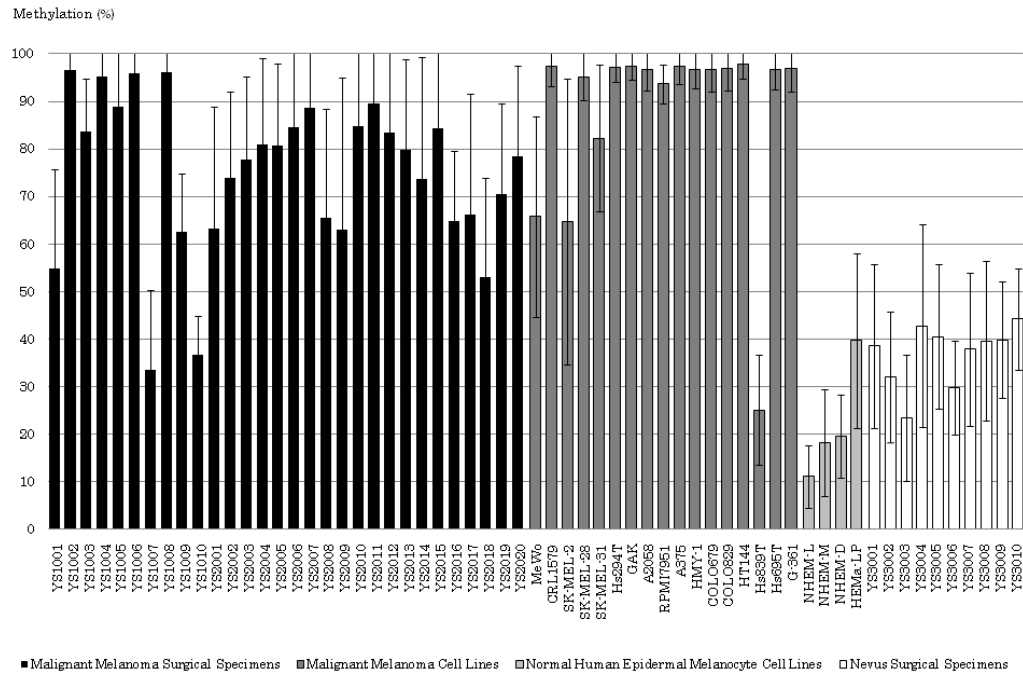
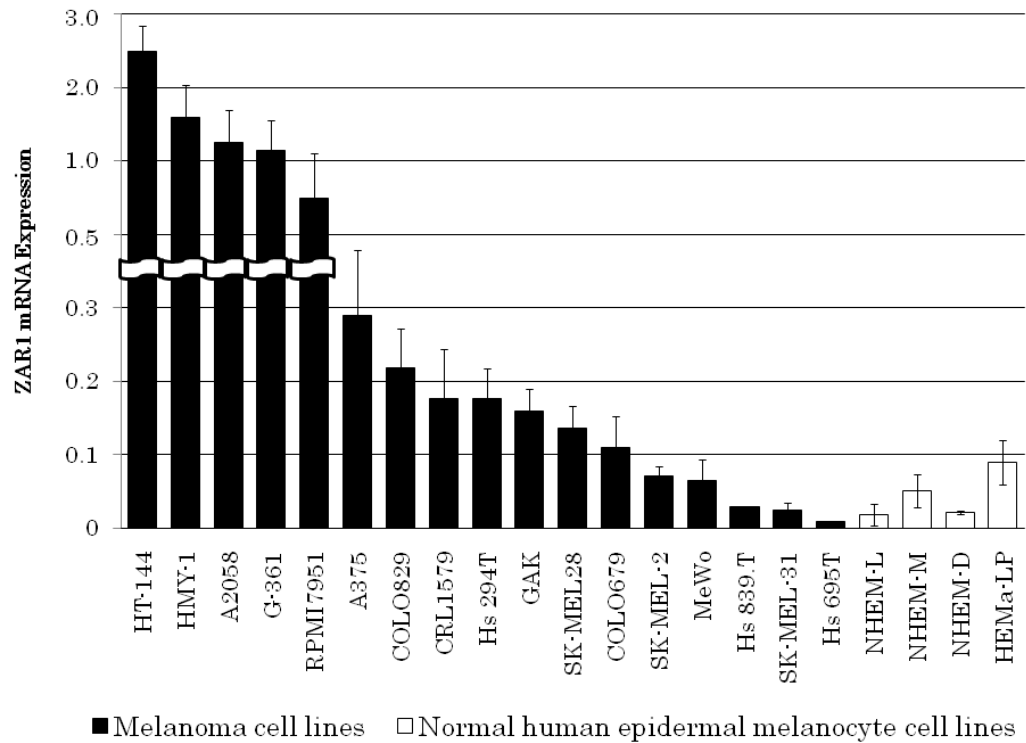
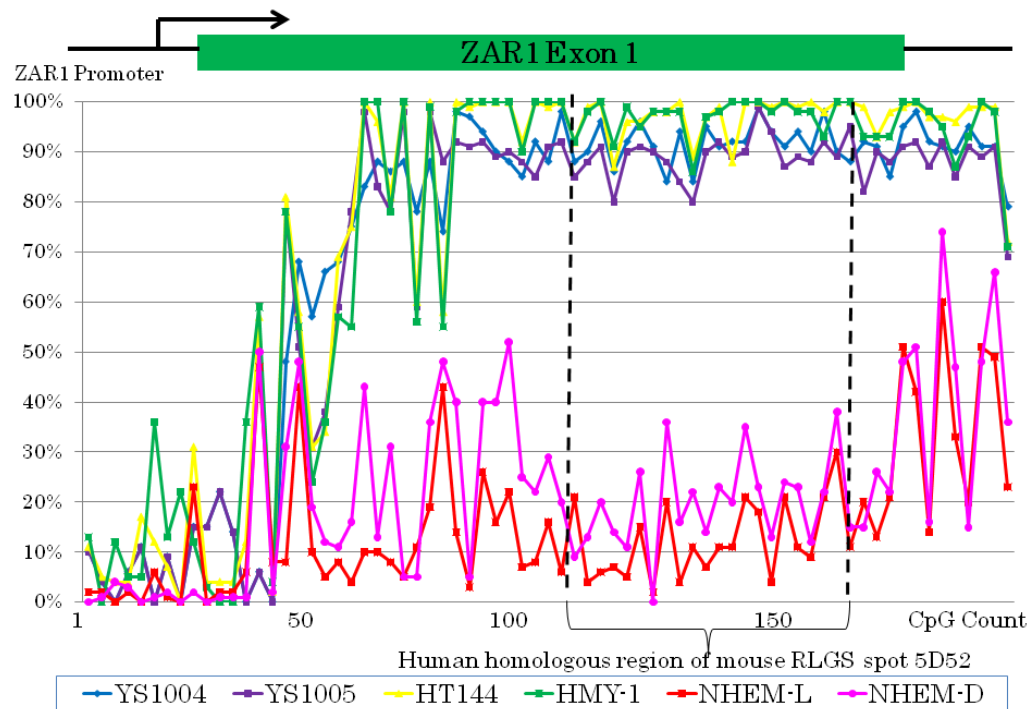


Fig. 2.
 Average of methylation levels for the entire target region of ZAR1.
 The y-axis represents the average of methylation levels for the entire 191 bp-target region of ZAR1-S-F and ZAR1-S-R primers amplified bisulfite-treated fragment (Table. S1). Error bars indicate the standard deviation of the mean.

**Fig. 3.**

ZAR1 gene expression.

Quantitative real-time PCR was performed to measure the mRNA expression of genes. The expression level was normalized to the GAPDH expression. The y-axis represents the normalized value determined by the standard curve of each gene. The expression level was calculated as the mean of three independent qRT-PCR data. Error bars indicate the standard deviation of the mean.

**Fig. 4.**

Methylation levels of the CpG island covered-over *ZAR1* promoter and Exon 1.

The bar graph indicates a quantitative measurement of the percent cytosine methylation levels at each CpG site within the entire CpG island covered-over *ZAR1* promoter and Exon 1. The blue and purple lines indicate malignant melanoma surgical specimens, YS1004 and YS1005, respectively. The yellow and green lines indicate malignant melanoma cell lines, HT-144 and HMY-1, respectively. The red and pink lines indicate normal human epidermal melanocyte cell lines, NHEM-L and NHEM-D, respectively.

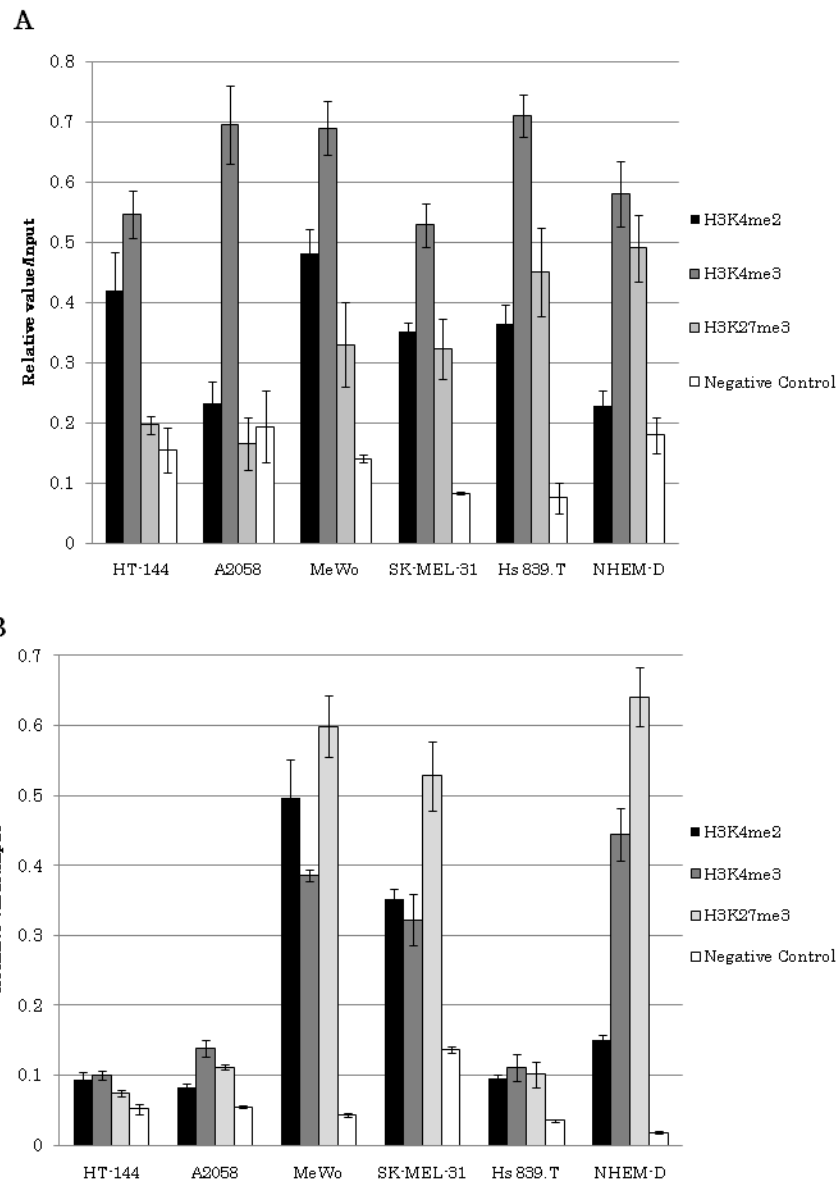


Fig. 5. Histone modifications at promoter region and Exon 1 region of ZAR1 in melanomas and normal melanocyte cells.
 A: Promoter region, B: Exon 1 region. The DNA fragment of the immunoprecipitated DNA was examined for the presence of histone modifications at a specific region by qRT-PCR. The y-axis represents the ratio of immunoprecipitated DNA to input. Error bars indicate the mean \pm standard deviation of three independent experiments.

Table 1

Aberrantly methylated regions in mouse-skin tumors identified by RLGs. Locus names are quoted from Smiraglia et al. [10], in which virtual RLGs information used in this study is described. The University of California, Santa Cruz Bioinformatics website was used for the genomic search.

No	Spot	Name	NotI site+1-200bp (UCSC July 2007)	%GC	CpG count	CpG Island	Cytogenetic Mapping	Gene Homology	Context	Function	Conserved human location (UCSC Mar. 2006)	Human gene	Description
1	10	2C 51	chr 10:53439336-53439735	78	62	Y	10qB3	AK015334	5'end	Hypothetical protein	chr6:119441525-119441671	FAM184A	Family with sequence similarity 184, member A
2	22	2D 48	chr4:6380704-6381103	73	50	Y	4qA1	Nsmaf	5'end	Couples p53TNF-receptor to neutral sphingomyelinase	chr8:59734679-59734998	NSMAF	Neutral sphingomyelinase (N-SMase) activation associated factor
3	34	4E 27	chr9:68452837-68453236	67	42	Y	9qC	Rora	5'end	Orphan nuclear receptor	chr15:59308408-59308815	RORA	RAR-related orphan receptor A
4	43	4C 14	chr14:62194710-62195109	75	39	Y	14qD1	Gata4	Body	Transcription factor GATA-4	chr8:11603427-11603785	GATA4	GATA binding protein 4
5	46	3B 16	chr6:8728002-8728401	74	43	Y	6qA1	Ica1	5'end	Islet cell autoantigen 1	chr7:8268180-8268513	ICA1	Islet cell autoantigen 1, 69kDa
6	103	3F 70	chr14:115809252-115809651	68	33	Y	14qE4	Gpc6	5'end	Putative cell surface coreceptor for growth factors, ECM proteins, proteases, anti-proteases	chr13:92678081-92678352	GPC6	Glypican6
7	105	3F 41	chr3:57935416-57935815	80	66	Y	3qD	Pfn2	5'end	Binds to actin and affects the structure of the cytoskeleton	chr3:151171326-151171762	PFN2	Profilin2
8	169	2G 50	chr12:68140755-68141154	71	43	Y	12qC2	Mamdc1	5'end	Cell-cell interaction	chr14:47214574-47214706	MDGA2	MAM domain containing glycosylphosphatidylinositol anchor 2
9	198	4F 46	chr11:53194404-53194803	66	47	Y	11qB1.3	Aff4	5'end	Transcription factor	chr5:132326842-132326980	AFF4	AF4/FMR2 family, member 4
10	212	3D 30	chr11:63739893-63740292	51	16	N	11qB3	Hs3st3b1	5'end	Transfers sulfuryl group	chr17:14142765-14143333	HS3ST3B1	Heparan sulfate (glucosamine) 3-O-sulfotransferase 3B1
11	213	4D 49	chr13:25277309-25277708	67	37	Y	13qA3.1	Vmp	5'end	Vesicular membrane protein	chr6:24234396-24234555	NRSN1	Neurexin 1
12	243	5D 36	chr4:48072835-48073234	70	32	Y	4qB1	Nr4a3	5'end	Binds to B1A response element	chr9:101630632-101630975	NR4A3	Nuclear receptor subfamily4, group A, member 3
13	255	3D 31	chr3:10070577-10070976	55	39	Y	3qA1	BC060946	5'end	Transcriptional repressor of the myelin basic protein gene	chr15:46248235-46248328	MYEF2	Myelin expression factor 2
14	280	5D 52	chr5:72860069-72860468	62	25	Y	5qC3.2	Zar1	5'end	Essential for female fertility. May play a role in the oocyte-to-embryo transition	chr4:48187102-48187970	ZAR1	Zygote arrest 1